Supplementary document to

Curvature tuning through defect-based 4D printing

Vahid Moosabeiki[a], Ebrahim Yarali[a,b], Ava Ghalayaniesfahani[a], Sebastien J. P. Callens[a], Teunis van Manen[a], Angelo Accardo[b], Sepideh Ghodrat[c], José Bico[d], Mehdi Habibi[e], Mohammad J. Mirzaali[a,*], Amir A. Zadpoor[a]

[a] *Department of Biomechanical Engineering, Faculty of Mechanical Engineering, Delft University of Technology (TU Delft), Mekelweg 2, 2628 CD, Delft, The Netherlands*
[b]*Department of Precision and Microsystems Engineering, Delft University of Technology, Mekelweg 2, 2628 CD Delft, The Netherlands*
[c]*Faculty of Industrial Design Engineering (IDE), Delft University of Technology (TU Delft), Landbergstraat, 15, 2628 CE Delft, the Netherlands*
[d]*Sorbonne Université, Université Paris Diderot and Laboratoire de Physique et de Mécanique des Milieux Hétérogenes (PMMH), CNRS, ESPCI Paris, PSL Research University - 10 rue Vauquelin, 75005 Paris, France*
[e]*Physics and Physical Chemistry of Foods, Department of Agrotechnology and Food Sciences, Wageningen University, 6708 WG, Wageningen, The Netherlands*

[*] Corresponding author. Tel.: +31-15-2783133
E-mail address: m.j.mirzaali@tudelft.nl

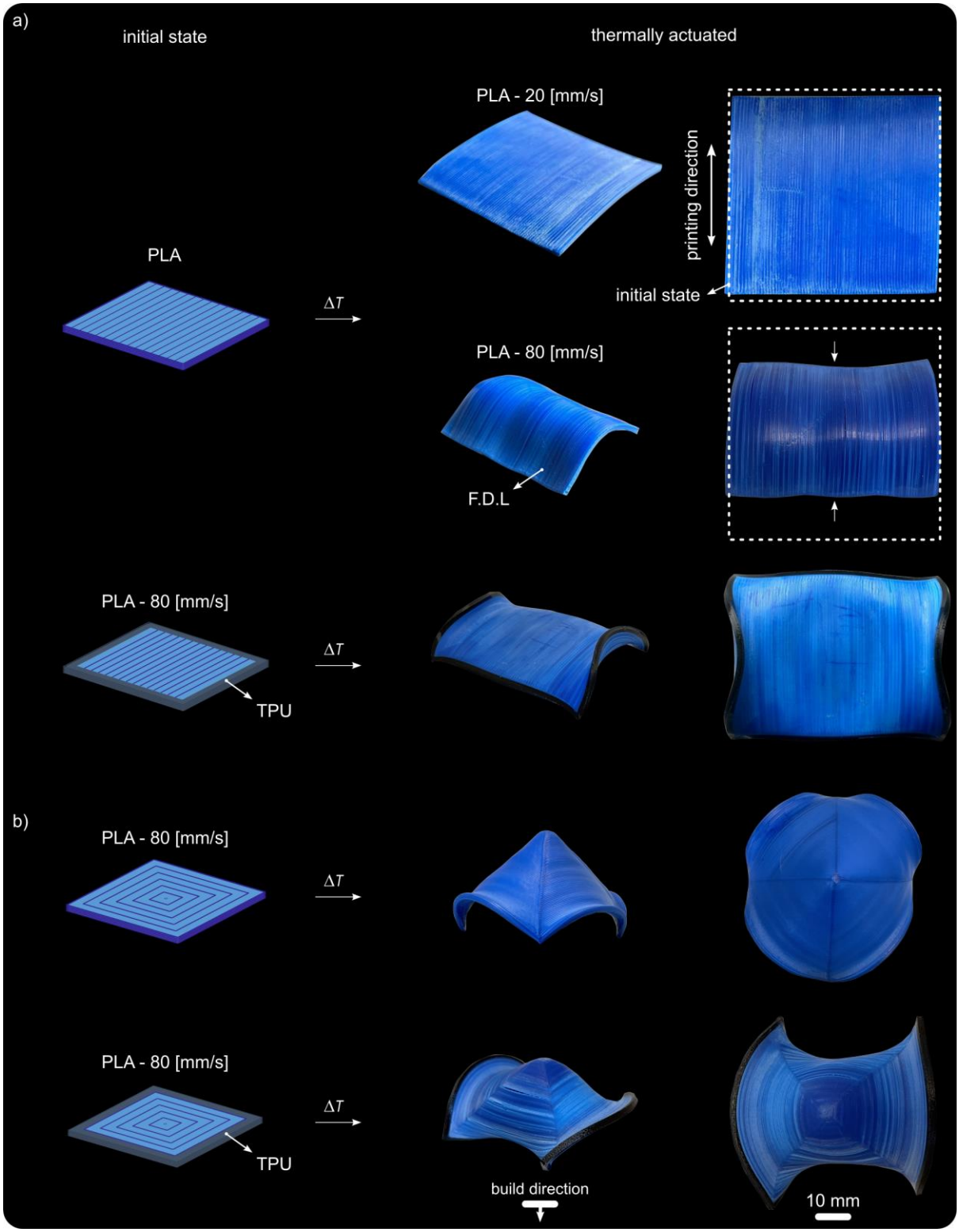

Supplementary Figure S1. The effects of distribution of residual stresses on the shape-shifting behavior of initially 4D printed square-shaped structures. PLA square plates were 3D printed at speeds of 20 and 80 mm s^{-1}, using linear patterns, and incorporating TPU (a), as well as using concentric patterns with and without TPU (b). All the specimens were printed with a uniform thickness of 2 mm. When a multi-material printing approach was used, $V_{PLA}/V_{total} = 90\%$ was maintained. The first deposited layers (F.D.L) are illustrated in (a) and (b).

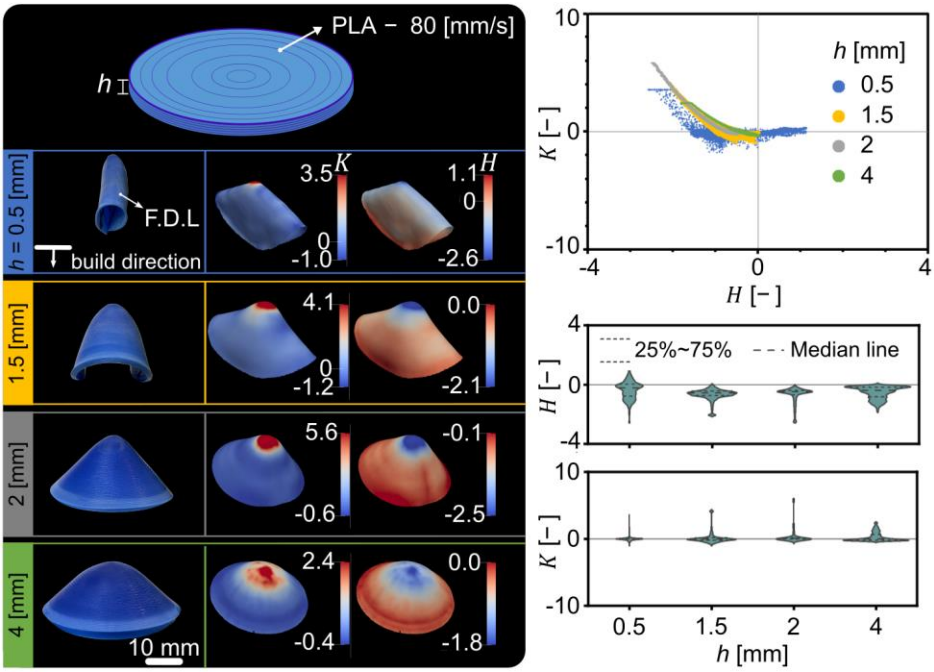

Supplementary Figure S2. The effects of the disk thickness (*h*) on the formation of the local curvature fields. PLA disks were printed at a speed of 80 mm s^{-1} with h = 0.5, 1.5, 2, or 4 mm. Throughout this study, the thickness of the disk was kept constant at h = 2 mm. The first deposited layers (F.D.L) are illustrated here.

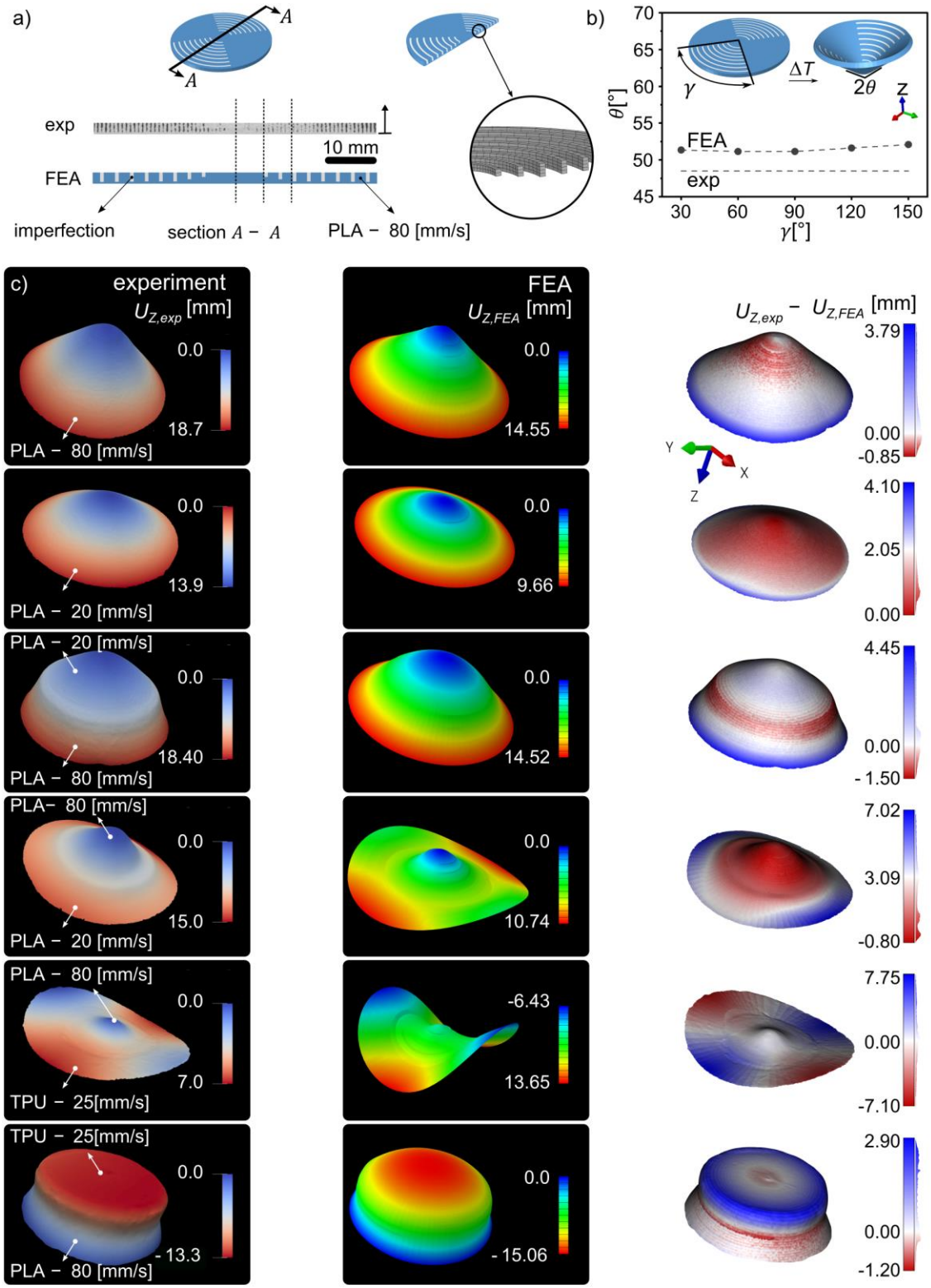

Supplementary Figure S3. The finite element analysis of imperfection-induced deformations in thermally actuated disks. The finite element analysis was used to predict the final shape of thermally actuated disks. The imperfections were introduced into the model by assigning extremely low material properties to the elements distributed in the radial, angular, and printing directions. The distribution of the voids was similar to what was observed in the μCT scans (a). The angular distribution of the imperfections (γ) does not have a marked effect on the out-of-plane deformations predicted by the model (b). The deformation obtained from our computational models agreed well with our experimental results (c).

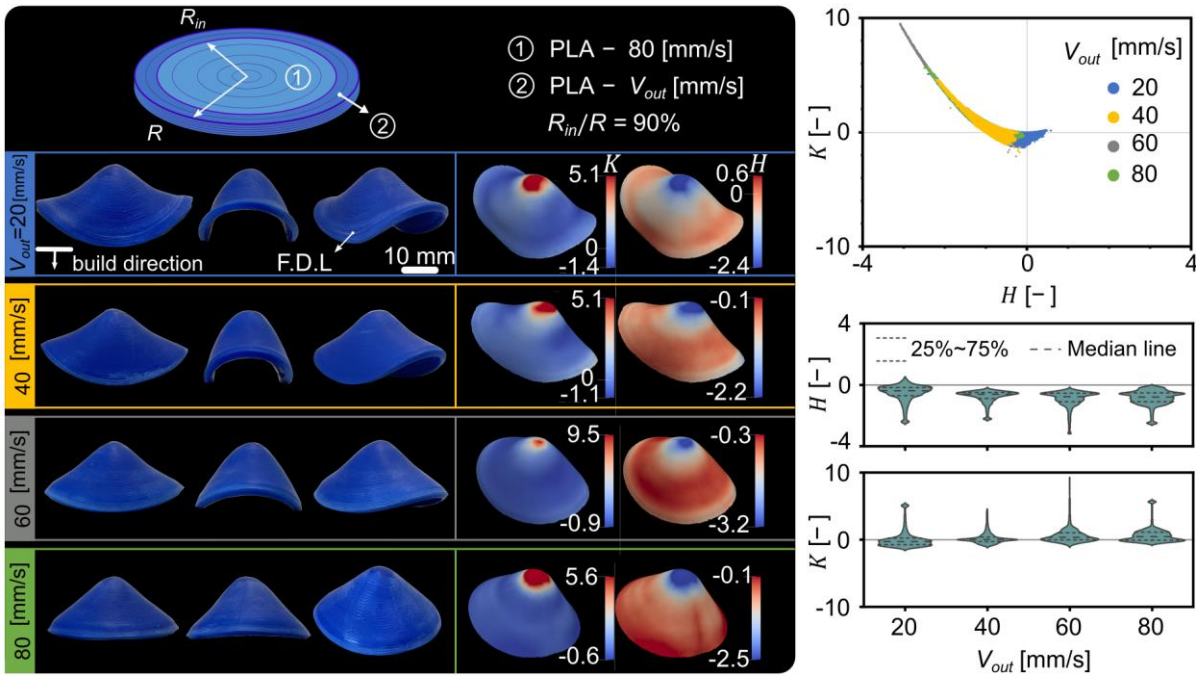

Supplementary Figure S4. The effects of printing speed in local curvature formations. The difference in the printing speed in the radial direction affects the formation of local curvatures. For the PLA disks with R_{in}/R = 90%, we decreased the printing speed of the outer layer (V_{out}) from 80 mm s^{-1} to 20 mm s^{-1}, which resulted in a higher level of local curvatures with a negative Gaussian curvature and a positive mean curvature (V_{out} = 20 mm s^{-1}). The first deposited layers (F.D.L) are illustrated here.

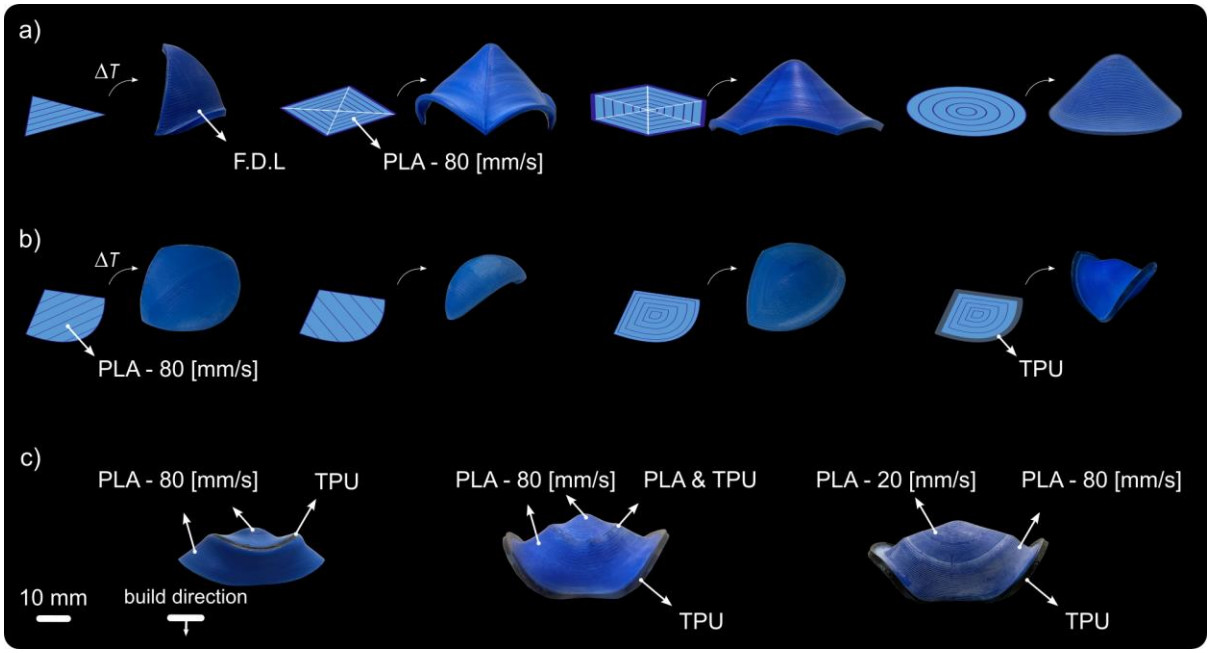

Supplementary Figure S5. The effects of initial shapes, printing patterns, and material depositions on the out-of-plane deformation of 4D printed structures. The out-of-plane deformation in 2D structures made from different initial shapes (*i.e.*, triangle with horizontal filament patterns, as well as square, hexagon, and circle with concentric filament deposition) showed similar dome-shape result after triggered by temperature (a). In these specimens, we used a printing speed of 80 mm s^{-1}. We further combined these shapes (*i.e.*, triangle and semi-circle) and 3D printed 2D planes with four different printing patterns including linear-horizontal, linear-vertical, concentric and the combination of concentric and multi-material (b). The printing pattern can significantly affect the out-of-plane results. We also showed how deposition of TPU can change the curvature that can be achieved during 4D printing (c). All specimens were 3D printed with an out-of-plane thickness of 2 mm. $V_{PLA}/V_{total} = 90\%$ was considered in multi-material specimens. The first deposited layers (F.D.L) are illustrated in (a–c)."

Supplementary Table S1. The thermal expansion coefficients for PLA and TPU materials which were used in the computational models.

Material	Thickness [mm]	Print speed [mm s^{-1}]	α_1 [$°C^{-1}$]	α_2 [$°C^{-1}$]	α_3 [$°C^{-1}$]
PLA	0.5	80	-0.00367	0.00023	0.00375
	1.5	80	-0.00367	0.00045	0.00233
	2	20	-0.00172	-0.00045	0.002
	2	80	-0.00346	-0.00068	0.002
	4	80	-0.00288	-0.00091	0.00162
TPU	2	25	-0.0002	-0.00002	0.0002

Supplementary Table S2. The temperature-dependent elastic moduli ($E(T)$) of PLA printed at 20 and 80 mm s^{-1} and TPU printed at 25 mm s^{-1}, which were used in our computational models.

Temperature [°C]	E [MPa]		
	PLA – 20 [mm s^{-1}]	PLA – 80 [mm s^{-1}]	TPU – 25 [mm s^{-1}]
40	2397.9	2334.67	58.234
43	2392.85	2325.14	56.820
46	2373.15	2304.41	55.383
49	2350.03	2284.69	53.866
52	2328.79	2258.1	52.411
55	2297.51	2220.38	50.917
58	2240.5	2151.83	49.457
61	2051.49	1986.19	47.970
64	1592.97	1619.69	46.463
67	928.349	1008.79	44.952
70	366.282	411.054	43.453
73	131.292	116.668	41.968
76	39.688	36.235	40.497
79	9.918	14.123	39.062
82	5.792	7.947	37.656
85	4.396	5.838	36.245
88	3.795	4.970	34.860
91	3.501	4.563	33.529
94	3.428	4.409	32.207
97	3.754	4.512	30.923
100	4.976	5.028	29.683